

The faint end of the Tully-Fisher relation

J.M. Stil¹ and F.P. Israel¹

Leiden Observatory, PO Box 9513, 2300 RA Leiden, The Netherlands

Received 11 September 1998; accepted 0000

Abstract. We have studied the relation between HI linewidth and optical luminosity in two samples of dwarf galaxies, with special attention to the accuracy of the inclination correction. The first sample consists of rotationally supported galaxies, and has DDO 154 as a prototype. They have HI linewidths significantly larger than predicted by an extrapolation of the Tully-Fisher relation. The deviation from the extrapolated Tully-Fisher relation correlates with the distance-independent mass-to-luminosity ratio $M_{\text{HI}}/L_{\text{B}}$. The baryonic correction for these gas rich galaxies is too small to explain the deviation from the Tully-Fisher relation, unless a small mass-to-light ratio $(M/L_{\text{B}})_{*} \leq 0.25$ for the stellar population is assumed. The second sample contains dwarf galaxies with comparable rotational and random velocities. This sample, having Leo A as a prototype, is consistent with an extrapolation of the classical Tully-Fisher relation to lower luminosities. These dwarf galaxies are not particularly rich in gas, but their mass is dominated by baryonic matter within their HI radius. We suggest that any evolution of the deviating galaxies towards the Tully-Fisher relation will combine a decrease in linewidth by radial transport of HI with an increase in luminosity due to a larger accumulated stellar mass.

Key words: Galaxies: irregular - structure - kinematics and dynamics - evolution

1. Introduction

The luminosity L and the rotational velocity v of a galaxy are empirically related by the so-called Tully-Fisher relation (Tully & Fisher 1977). Simple arguments lead to the general form $L \sim v^4$, although the value of the exponent depends on the filter in which L is measured as well as the manner of determining the rotational velocity v (Verheijen 1997). Although it is often assumed that the relation is strictly linear in a logarithmic sense, there is no reason why this should apply to all galaxies.

A useful reference frame is provided by the Tully-Fisher relation from Kraan-Korteweg et al. (1988), fitted to a sample

of 13 nearby galaxies in the luminosity range $-16.4 > M_{\text{B}} > -21.7$:

$$M_{\text{B}} = -6.69 \log \Delta v_{21} - 2.77 \quad (\pm 0.1) \quad (1)$$

where Δv_{21} is the *inclination-corrected* width of the 21 cm HI line profile at 20% of the peak value; we reserve the symbol W_{20} for the *observed* linewidth at 20% of the peak value. The calibration of this relation corresponds to a Hubble constant $H_0 = 56.6 \text{ km s}^{-1} \text{ Mpc}^{-1}$. Kraan-Korteweg et al. (1988) have compared this relation to the Tully-Fisher relation defined by different types of galaxies in the Virgo cluster. The dwarf galaxies discussed here are considerably fainter than any of the galaxies considered by Kraan-Korteweg et al. (1988). We must therefore extrapolate the Tully-Fisher relation to lower luminosities. As an example, a galaxy with linewidth $\Delta v_{21} = 50 \text{ km s}^{-1}$ is thus predicted to have a luminosity $M_{\text{B}} \approx -14$.

In the literature, observations exist of half a dozen dwarf galaxies fainter than $M_{\text{B}} = -14.5$, with rotational velocities up to 50 km s^{-1} (i.e. $\Delta v_{21} \approx 100$) and with reliable distances (DDO 154: Carignan & Beaulieu 1989; DDO 161, UGCA 442, ESO381-G20: Côté et al. 1997; DDO 87: Stil & Israel, in preparation). Until now, only two objects were known to deviate by a large amount from the extrapolated Tully-Fisher relation: DDO 154 (Carignan & Beaulieu 1989) and the more luminous starburst dwarf NGC 2915 (Meurer et al. 1996). Both have luminosities lower than expected from their linewidth and the T-F relation. Although Zwaan et al. (1995) found no difference between the T-F relations pertaining to more luminous low-surface brightness galaxies and to high-surface brightness galaxies, Matthews et al. (1997) concluded that extreme late-type galaxies also are systematically fainter than inferred from the T-F relation and their linewidth. Furthermore, Matthews et al. (1997) found the baryonic correction, i.e. a correction to the luminosity to account for the large gas fraction in these galaxies, too small to explain the observed deviation.

Here we present two samples of dwarf galaxies, all observed in detail with a radio interferometer, extending the low-luminosity limit to $M_{\text{B}} = -13$ and -10 respectively. The first, containing galaxies clearly dominated by rotation, deviates significantly from the extrapolated T-F relation. In contrast, the

Send offprint requests to: J.M. Stil

Correspondence to: stil@strw.leidenuniv.nl

second sample of dwarf galaxies with considerably smaller rotational velocities does not, at least over the same luminosity range. The physical differences between the two samples are discussed.

2. Sample selection

2.1. General considerations

We have studied two samples of dwarf galaxies which are distinguished by their kinematic properties: (1). dwarf galaxies with a regular velocity field, kinematically well-described by tilted ring models, and (2). dwarf galaxies rotating so slowly that the random motions of the HI are dynamically important. As the dynamical mass is roughly proportional to $R_{\text{HI}}v^2$, where R_{HI} is the radius of the HI distribution and v is the rotation velocity at that radius, these samples are also expected to be different in dynamical mass. Sample galaxy distances were taken from published stellar photometry or published group membership. Hubble expansion and a correction for Virgocentric infall were adopted for a small fraction of the sample.

Galaxy linewidths W_{20} were taken from Bottinelli et al. (1990), insuring that the corrections for instrumental resolution and primary beam dilution were performed in the same way for all objects.

2.2. Rotation curve (RC) sample

The first sample consists of galaxies with an accurately measured rotation curve. The selection criteria for this rotation-curve sample were: (1). the rotation curve can be determined by a tilted-ring analysis; (2). the rising part of the rotation curve is well resolved; (3). the inclination can be included in the fit as a free parameter.

The use of a tilted ring analysis does not allow inclusion of objects with an inclination $i < 50^\circ$ and objects with a solid-body rotation curve, as their inclination cannot be determined from the tilted ring fit. The advantage of obtaining kinematic inclinations is that it avoids assumptions about the poorly known intrinsic axial ratios of these objects. Nevertheless, we have included in Table 1 four dwarf galaxies with considerable rotational velocity for which the inclination could not be determined from a tilted ring fit. For these inclinations were estimated from the ellipticity of the HI isophotes. One of these galaxies, DDO 47 is a particularly good example of a galaxy with a solid-body rotation curve.

Although we limit our analysis to the dwarf galaxies in this sample, i.e. galaxies with $M_B > -16$, we have also included in Table 1 a number of more luminous galaxies for comparison purposes.

2.3. Slow-rotation (SR) sample

The second sample is based on our aperture synthesis radio observations of “classic” dwarf galaxies which exhibit little or no rotation, very different from the rotation-curve (RC) sample

discussed above. The selection criterion for this sample is low observed maximum *projected* rotation velocity $V_{\text{max}} \sin(i) < 25 \text{ km s}^{-1}$. Since the faint dwarf galaxies studied by Lo et al. (1993) also obey this criterion, they are included in the sample.

The selection on *projected* rotation velocity neglects the effects of the uncertain inclination of these objects. The sample may thus be contaminated by some fast-rotating face-on galaxies, but we are confident that we can identify these by the large inclination correction implied by their axial ratios. The resulting slow rotators are listed in Table 2. A lower limit of 30° to the inclination is adopted. A justification for this limit is given in Section 3.

We did not constrain the luminosity of the galaxies in this sample. The luminosities of the slow rotators, which may be as low as $M_B = -10$, in fact overlap with the RC sample in the range $-12 > M_B > -16$. The three faintest slow rotators are objects from the sample of Lo et al. (1993).

2.4. Comments on structure

Some general remarks about the HI and optical structure of the dwarfs in the two samples can be made.

The dwarf galaxies in the RC sample usually have a large HI disc with modest HI column densities surrounding the optical galaxy. A representative example is DDO 154 (Carignan & Beaulieu 1989).

The HI distribution of the slow rotators DDO 63, DDO 69, DDO 125, and DDO 165 is characterized by a small number of regions with higher HI column density, usually in a ring or a ridge, around the edge of the optical galaxy. A smaller HI column density is observed near the centre. DDO 63, DDO 69 and DDO 125 appear to have an extended HI halo with a low HI column density. DDO 69 (Young & Lo 1996) is a representative example. DDO 22 is suggested as an edge-on slow rotator because of its elongated HI distribution and its similar appearance on the POSS plates.

3. Correction for inclination

The actual HI linewidth Δv_{21} of a galaxy is a complex combination of the rotation curve, the gas distribution and the relative importance of an isotropic component. The observed linewidth is smaller as a result of projection onto the plane of the sky.

These factors are of minor importance in large spiral galaxies where generally a symmetric HI disc extends far beyond the radius where the rotation curve reaches its high, constant value. In contrast, the gas distribution and HI velocity dispersion are important in dwarf galaxies which have a rising rotation curve and a low overall rotation velocity. Effects of the HI distribution on HI linewidths were studied before by Shostak (1977).

The relation between the observed linewidth W_{20} and the intrinsic linewidth Δv_{21} is straightforward if the rotational velocity is much larger than the isotropic random motions, so that $W_{20} \approx \Delta v_{21} \sin(i)$. More in general, however, a correction for the contribution of random motions cannot be avoided. This is often done in a statistical way described by Tully & Fouqué

Table 1. Rotation curve sample with fast rotators

Name	dist	M _B	B-V	h	R _{max}	V _{max}	< σ >	Type	i	Δv_{21}	M _{HI} /L _B	log(M _{VT} /β)	ref
[1]	[2]	[3]	[4]	[5]	[6]	[7]	[8]	[9]	[10]	[11]	[12]	[13]	[14]
DDO 87	3.4	-12.8	0.26		2.0	34.4	6.0	Im	63 ± 2	82	2.6	8.77	a
DDO 154	4	-13.8	0.37	0.50	7.6	43.1		IBm(s)	64 ± 3	109	5.5	9.57	c *
UGCA 442	2.5	-13.8	0.29	0.43	3.6	54.4	8.4	SBm(s)(sp)	70 ± 10	120	1.6	9.43	m *
ESO381-G20	3.5	-13.9	0.3	0.62	3.7	62.8	8.7	IBm(s)	58 ± 4	121	1.7	9.56	m *
DDO 83	9	-14.5	0.01	0.65	3.3	51.0	10.0	IBm(s)	53 ± 2	150	2.4	9.34	a
DDO 170	12	-14.5	0.4	1.30	11.7	62.2		Im	70 ± 3	82	4.8	10.05	d *
DDO 161	3.5	-14.9	0.29	0.70	6.2	64.4	9.3	IBm(s)	68 ± 5	147	2.3	9.80	m *
UGC 7906	16	-15.0	0.43	1.24	4.6	55		Im	50 ± 5	151	1.6	9.54	k *
DDO 168	3.5	-15.2	0.22	0.92	3.4	48.7	10.6	IBm	61 ± 1	90	1.1	9.33	a,b *
IC 3522	16	-15.6	0.53	1.62	6.9	57.0		IBm	70 ± 5	128	2.2	9.75	k *
NGC 1560	3.0	-15.9	0.57	1.3	8.3	76.6		SAd(sp)	80 ± 3	159	2.5	10.07	b *
NGC 2915	5.3	-15.9	0.39	0.66	14.1	87.0	12.0	IO	57 ± 2	199	2.9	10.42	h *
DDO 48	16	-16.4	0.59	1.78	8.0	76.6	10.1	Sm	80 ± 4	168	1.3	10.06	a
NGC 3109	1.7	-16.8		1.55	8.2	65.7		SBm(s)	70 ± 5	128	1.7	9.94	n *
IC 3365	16	-17.0	0.52	1.58	4.6	58		Im	70 ± 5	156	0.3	9.58	k *
UGC 4278	6.4	-17.3	0.40		4.7	87.6		SBd(sp)	90	201	0.35	9.94	a
NGC 2976	3.4	-17.4	0.58	1.07	2.0	71.5	11.8	SAdP	66 ± 2	183	0.11	9.41	a
NGC 5585	6.2	-17.5	0.47	1.4	9.7	89.4		SABd(s)	52 ± 2	209	1.1	10.26	i *
NGC 300	1.8	-17.9	0.58	2.06	10.6	93.4		SAd(s)	52 ± 8	190	0.33	10.34	f *
NGC 247	2.5	-18.0	0.54	2.93	9.8	107.8		SABd(s)	74 ± 3	229	0.34	10.43	e *
DDO 105	16	-18.1	0.53		15.1	81.8		IBm(s)	64 ± 2	187	0.8	10.38	b
M 33	0.72	-18.6	0.47	1.7	5.4	106.8		Scd	54	251	0.24	10.16	l
Dwingeloo 1	3	-19.0			6.4	109		SBb	51 ± 2	262	0.073	10.27	j
NGC 2403	3.0	-19.3	0.39	2.05	19.5	134		SABcd(s)	60 ± 2	302	0.39	10.91	g *
NGC 3198	9.4	-19.4	0.43	2.60	10.9	153		SBc(rs)	74 ± 3	332	0.56	10.78	g *
NGC 2903	6.4	-20.0	0.55	2.02	14.9	188		SABbc(rs)	63 ± 3	429	0.16	11.09	g *
NGC 801	79	-21.7	0.61	12	59	216		Sc	75 ± 1	468	0.30	11.8	b *
DDO 47	2	-13.4	0.35	0.5	1.6	67.0	8.7	IBm(s)	30 (HI)	158	1.8	9.24	a
DDO 52	5.3	-13.8	0.53	0.6	3.0	52.9	7.4	Im:	55 (HI)	123	1.1	9.31	a
DDO 68	6.1	-14.3	0.23	0.5	3.5	54.7	12.6	Im pec	57 (HI)	116	2.9	9.45	a
DDO 64	6.1	-14.7	0.15	1.2	2.7	41.8	10.9	Im	80 (HI)	110	1.2	9.11	a

Column definitions : [1] Object name; galaxies are ordered by luminosity; objects below the horizontal line have no kinematic estimate of the inclination; [2] distance in Mpc; [3] absolute magnitude in B; [4] B-V colour; [5] exponential disc scale length (from the rotation curve reference); [6] radius of the last measured point of the rotation curve in kpc; [7] velocity of the last measured point of the rotation curve in kpc; [8] mean HI velocity dispersion; [9] galaxy type from RC3; [10] inclination from the tilted ring fit in degrees; [11] Full width of the 21 cm line profile at 20 % of the peak divided by $\sin(i)$, in km s^{-1} . Linewidths were taken from (Bottinelli et al. (1990)); [12] ratio of HI mass to B luminosity in $M_{\odot}/L_{B\odot}$; [13] $\log(\beta^{-1}(M_{VT}/10^8 M_{\odot}))$ from equation (3); [14] references to rotation curve data : a Stil & Israel (in preparation); b Broeils (1992); c Carignan & Beaulieu (1989); d Lake et al. (1990); e Carignan & Puche (1990); f Puche et al. (1990); g Begeman (1987); h Meurer et al. (1996); i Côté et al. (1991); j Burton et al. (1996); k Skillman et al. (1987); l Newton (1980); m Côté et al. (1997); n Jobin & Carignan (1990). Detailed mass models exist in the literature for the galaxies indicated with *

(1985). As this correction works in the direction of the effect described in Section 4.1, and therefore might introduce spurious systematic differences between the two samples, we have chosen not to apply it. Instead, we will model the magnitude of the effects due to gas distribution, random motions and inclination on the observed widths of the line profiles. In order to do so, we have constructed a set of Monte Carlo model observations of dwarf galaxies with the GIPSY program GALMOD (originally written by T.S. van Albada). A model observation is based on a rotation curve, an axially symmetric HI distribution and the velocity dispersion of the HI gas. An HI layer with finite thickness can be modeled. We adopted an exponen-

tial vertical profile with a scale height above the plane of 10% of the HI radius. Changes in this scale height by factors of up to two do not change our results within the statistical noise.

The model is built up of clouds consisting of a large number of subclouds with no intrinsic velocity dispersion. Cloud positions and velocities, as well as subcloud velocities are produced by a random generator in a model data cube according to the specifications of the gas distribution, rotational velocity, local velocity dispersion, scale height and projection parameters (position angle and inclination). The parameters which define the random realizations are the number of annuli, the number of clouds per annulus, the number of subclouds within

Table 2. Slow-rotation sample

Name	dist	M_B	B-V	Type	i	src	W_{20}	R_{\max}	$V_{\max} \sin(i)$	M_{HI}/L_B	$\log(M_{\text{VT}}/\beta)$	ref
[1]	[2]	[3]	[4]	[5]	[6]	[7]	[8]	[9]	[10]	[11]	[12]	[13]
LGS 3	0.76	-9.2	0.7	I?	34	opt	36	0.5	< 2	0.28	6.73	b
DDO 210	1.0	-9.9	0.08	IAm	45	opt	31	0.3	< 5	2.21	6.84	b
Sag DIG	1.1	-10.6	0.4	IBm(s)	40	opt	31	0.8	< 2	3.10	7.00	b
M81 dw A	4.6	-12.4	0.4	I?	37	opt	33	1.0	2.5 ± 1	0.81	7.67	g
UGC 4483	3.25	-13.0		Im:	30	opt	56	1.0	10 ± 2	1.1	8.09	b
DDO 216	1	-13.1	0.62	Im	58	opt/HI	35	0.6	7 ± 5	0.15	7.32	a,b
DDO 69	1.5	-13.5	0.31	IBm	59	opt/HI	46	1.1	< 2	0.96	7.30	b,f
DDO 75	1.7	-13.8	0.37	IBm(s)	36	opt/HI	62	1.2	20 ± 5	1.18	8.57	d
DDO 187	4.0	-13.8	0.38	Im	37	opt	49	1.1	< 5	1.02	7.79	b
IC 1613	0.725	-14.4	0.67	IBm(s)	38	opt/HI	35	2.6	12 ± 2	0.70	8.50	e
DDO 22	9.9	-14.9	0.09	Im:	90	HI	67	2.9	19 ± 3	1.04	8.68	a
DDO 63	3.4	-15.0	-0.09	IABm(s)	42	HI	44	2.5	8.6 ± 3	0.73	8.34	a,c
Mkn 178	5.2	-15.0	0.35	Im	56	opt	47	1.1	~ 6	0.12	7.65	a
DDO 125	4.5	-15.6	0.40	Im	50	opt/HI	46	2.6	11 ± 3	0.41	8.35	a,c
DDO 165	4.6	-15.8	0.23	Im	38	opt/HI	62	1.9	26 ± 7	0.33	9.00	a

Column definitions: [1] Object name; DDO 63 = Holmberg I; DDO 69 = Leo A; DDO 75 = Sex A; IC 1613 = DDO 8; [2] distance in Mpc; [3] absolute magnitude in the B band; [4] B-V colour; [5] galaxy type from RC3; [6] inclination in degrees; [7] source of the inclination : opt = optical axial ratio, HI = HI axial ratio; assumed intrinsic axial ratio is $q_0 = 0.15$ as explained in the text; [8] width of 21 cm line profile at 20 % of the peak in km s^{-1} , without inclination correction; [9] measured maximum rotation velocity without inclination correction; [10] ratio of HI mass to B luminosity in $M_\odot/L_{B\odot}$; [11] $\log(\beta^{-1}(M_{\text{VT}}/10^8 M_\odot))$ from equation (3); [12] references : a Stil & Israel (in preparation) ; b Lo et al.(1993); c Tully et al. (1978); d Skillman et al. (1988); e Lake & Skillman (1989); f Young & Lo (1996); g Sargent et al. (1983)

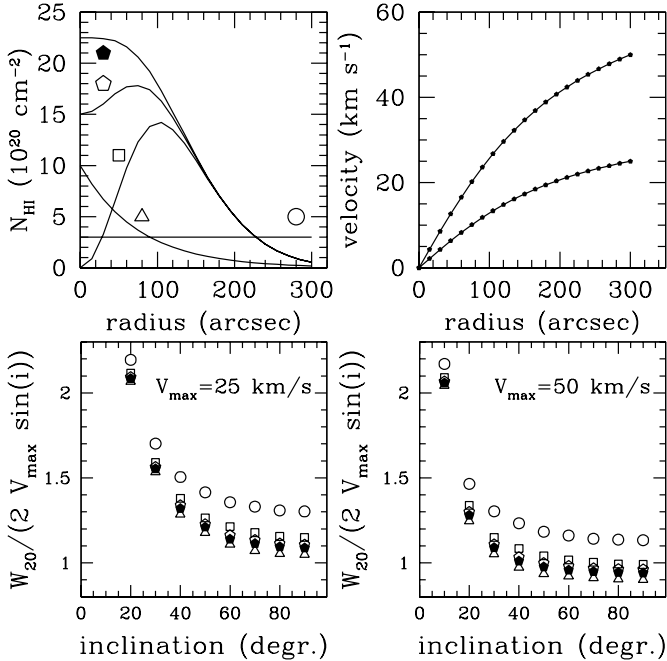


Fig. 1. Galaxy total HI linewidths as a function of inclination for two sets of Monte Carlo models. Each set consists of five radial HI distributions shown at top left, and a rotation curve shown at top right. Bottom panels show the ratio of $W_{20}/(2V_{\max} \sin(i))$ as a function of inclination. In the absence of an isotropic component, this ratio would be constant.

each cloud and the initialization of the random generator. As

we are interested in the *integrated* line profile, the results presented here are not sensitive to the number of clouds in a single ring. The statistical noise in the linewidth W_{20} as determined from different random realizations of the same model, is of the order of 0.1 km s^{-1} . The models were calculated on a grid of $5'' \times 5'' \times 4.12 \text{ km s}^{-1}$, identical to the sampling of our WSRT observations (Stil & Israel, in preparation). The flux of the model in each of the individual velocity channels yields the model line profiles. The models contain 20 concentric annuli each, with 5 clouds per 10^{20} cm^{-2} HI column density and 1000 subclouds per cloud to define the internal velocity structure. Experiments with larger numbers of clouds produced similar linewidths to within 0.1 km s^{-1} .

The rotation curve of an isothermal sphere was used to define the rotation velocity as a function of radius. This is an accurate representation for the shape of the rotation curves of dwarf galaxies (Kravtsov et al. 1998, Stil & Israel 1998). Thus:

$$v(r) = V_0 \frac{r_c}{r} (1 - \arctan(\frac{r}{r_c}))$$

The core radius r_c and the maximum rotation velocity V_0 were varied independently. A solid body rotation curve corresponds to $r_c \gg R_{\text{HI}}$, a flat rotation curve with $r_c \ll R_{\text{HI}}$. The models discussed here have rotation curves with $r_c = 0.5 R_{\text{HI}}$ and maximum rotational velocities of 25 km s^{-1} and 50 km s^{-1} respectively.

All models were calculated with a line of sight velocity dispersion of 9 km s^{-1} . This is the mean velocity dispersion in our WSRT sample of dwarf galaxies.

Five shapes for the radial HI distribution were considered. These are shown in Fig. 1. The profiles represent different HI

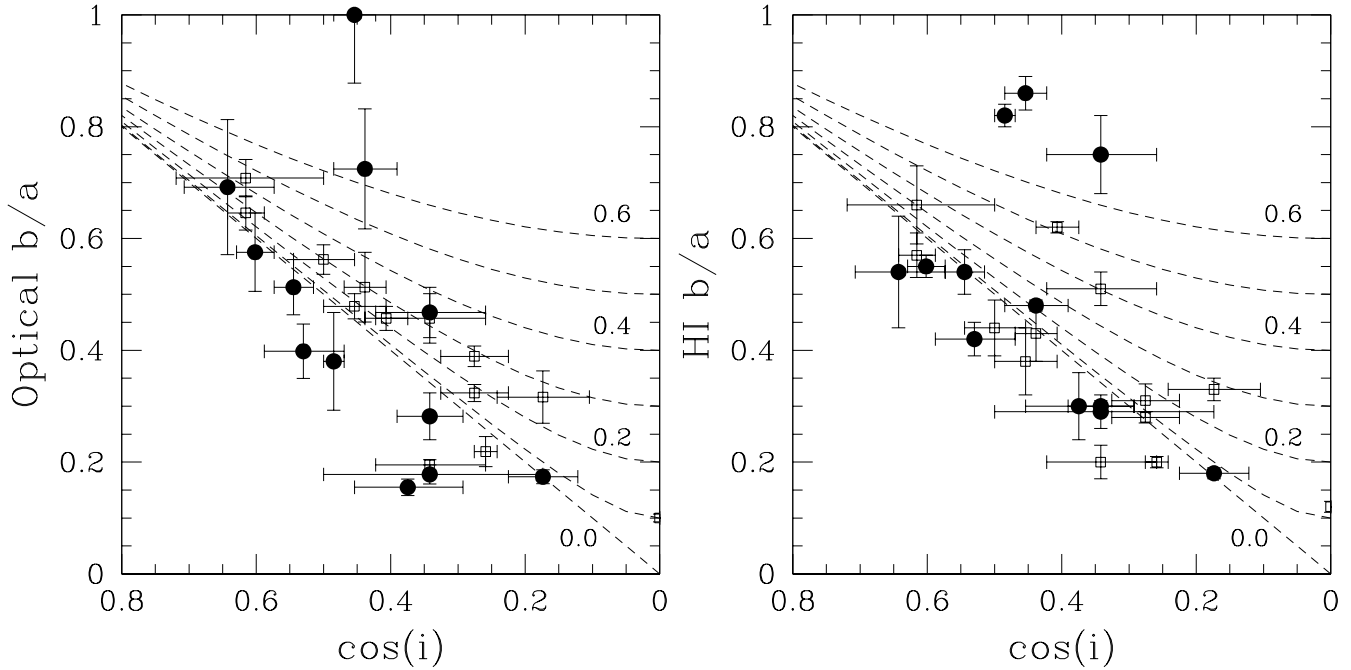


Fig. 2. Optical axial ratios (top) and HI axial ratios (bottom) as a function of $\cos(i)$ for the rotation curve sample. Inclination increases from left to right. Filled circles indicate the dwarfs ($M_B > -16$), open squares the more luminous galaxies. Dashed lines show observed axial ratios as a function of $\cos(i)$ according to equation (1) for intrinsic axial ratios 0, 0.1, 0.2, ..., 0.6.

column density profiles in our sample. The shape of the line profile, and therefore its width at a percentage of the peak, are not affected by the normalization of the column density. Therefore, we treat the rotation curve and the gas distribution independently.

Each model was evaluated for inclinations 10 to 90 degrees at 10 degree intervals. Model W_{20} linewidths relative to the projected maximum rotation velocity are plotted in Fig. 1. If the isotropic velocity component can be neglected, the ratio $W_{20}/(2V_{\max} \sin(i))$ depends only on the gas distribution and the shape of the rotation curve. Centrally concentrated distributions, such as an exponential profile (triangles in Fig. 1), result in linewidths about 30% lower than those reflecting a homogeneous distribution (circles).

If the isotropic component (i.e. the line of sight velocity dispersion which we kept at 9 km s^{-1}) contributes significantly to the observed linewidth, the ratio $W_{20}/(2V_{\max} \sin(i))$ increases. This is illustrated in Fig. 1 which shows the linewidths for two different rotation curves. The ratio $W_{20}/(2V_{\max} \sin(i))$ is significantly larger for the $V_{\max} = 25 \text{ km s}^{-1}$ rotation curve; the difference increases with decreasing inclination. The scatter introduced by the HI distribution is approximately 15%. Within this scatter, the approximation $\Delta v_{21} \approx W_{20}/\sin(i)$ does not introduce a significant error if the inclination $i > 50^\circ$ and $V_{\max} > 25 \text{ km s}^{-1}$. At inclinations between 30 and 50 degrees, the increase in $W_{20}/(2V_{\max} \sin(i))$ remains small for the models with $V_{\max} \approx 50 \text{ km s}^{-1}$, but for those with $V_{\max} \approx 25 \text{ km s}^{-1}$, only upper limits to Δv_{21} are obtained.

The models show that a straightforward inclination correction $1/\sin(i)$ may be applied to dwarfs with rotation veloci-

ties as low as 25 km s^{-1} provided $i > 50^\circ$. A more advanced method requires the inclusion of the gas distribution in the inclination correction, which is beyond the scope of this paper.

The Monte Carlo models, of course, do not include the uncertainty in the inclination itself, which is difficult to measure. The least biased method is to fit the inclination as a free parameter in a tilted ring analysis of the velocity field. This is not possible if the rotation velocity is small or if the rotation curve increases linearly with radius. In those cases, we use

$$\cos^2(i) = \frac{q^2 - q_0^2}{1 - q_0^2} \quad (2)$$

with the intrinsic axial ratio $q_0 = 0.15$. Such a small axial ratio may not be realistic for dwarf galaxies (cf. Staveley-Smith et al. 1992), but it is a reasonable lower limit to the true axial ratio of any dwarf galaxy. Inclination corrections $1/\sin(i)$ thus derived are therefore upper limits. For prolate galaxies, this method would yield erroneous inclinations. However, most of the observed galaxies exhibit good alignments of the optical, HI and kinematic major axes, which suggests that this situation does not apply.

In order to verify the quality of the inclination corrections so obtained, we have verified that they agree with the kinematic inclinations derived for the rotation-curve sample. As HI axial ratios are seldom given in the literature, we measured the axial ratio of the contours near the level $N_{\text{HI}} = 2 \cdot 10^{20} \text{ cm}^{-2}$ in HI column density maps in the references of the rotation curves. The optical axial ratios were taken from the Third Reference Catalogue (de Vaucouleurs et al. 1991). Fig. 2 shows the relation between the observed axial ratio and the kinematic in-

clination for the rotation curve sample. The result shows both axial ratios and $\cos(i)$ to be well-correlated, as expected for flattened systems. The correlation suggests intrinsic axial ratios $b/a \leq 0.3$. A few dwarfs have observed axial ratios slightly smaller than those expected for an infinitely thin system with the same inclination.

Some other dwarfs show departures from the correlation which are consistent with a larger intrinsic axial ratio. However, deviations from axial symmetry and variation of the intrinsic axial ratios q_0 have similar consequences in Fig. 2. The objects with the most extreme HI axial ratio are DDO 87, DDO 168, and IC 3522. DDO 168 and IC 3522 also have optical axial ratios which are approximately half their HI axial ratio. We nevertheless conclude that the optical and HI axial ratios are consistent with the kinematic inclination for the majority of the galaxies in the RC sample.

The derived value of Δv_{21} is an upper limit for the slow rotators, as the rotation velocity is small and the inclination is derived from the observed axial ratio. For the fast rotators, $\Delta v_{21} = W_{20}/\sin(i)$, within the limits discussed above and the inclination is derived from the tilted ring fits.

4. Results

4.1. The Tully-Fisher relation for the two samples

The relation between W_{20} and M_B for the fast rotators is shown in Fig. 3. The reference frame is provided by the Tully-Fisher relation for a sample of local calibrating galaxies with luminosity $-16.4 > M_B > -21.7$ and a sample of Virgo cluster galaxies from Kraan-Korteweg et al. (1988). The open symbols represent the linewidths before the inclination correction. The inclination-corrected linewidths are shown as filled circles.

If random motions contribute significantly to the width of the 21 cm line, the widely derived line of sight velocity dispersion $\sigma \approx 10 \text{ km s}^{-1}$ implies that the linewidth should be $\Delta v_{21} = W_{20} = 36 \text{ km s}^{-1}$ in the limit of zero rotation velocity and isotropic random motions with a gaussian velocity distribution.

Essentially all galaxies in the rotation-curve sample with relatively high luminosities $M_B < -17$ follow the Tully-Fisher relation. The most luminous sample galaxy (NGC 801) falls within the scatter defined by the Virgo galaxies. In contrast, the fainter rotation-curve sample galaxies deviate from the extrapolated T-F relation. They either are underluminous or have a larger linewidth than expected from this relation. This is even the case if we use W_{20} linewidths corrected for instrumental resolution but not for inclination. We may therefore rule out that this deviation is an artifact caused by the inclination correction. In addition, the maximum rotation velocity of the fast rotators is well above 50 km s^{-1} and we showed in Section 3 that errors introduced by ignoring the contribution of random motions to the linewidth are small for such galaxies.

DDO 168 is the only dwarf galaxy in the rotation-curve sample that is consistent with the extrapolation of the T-F relation, thereby breaking the pattern established by the other

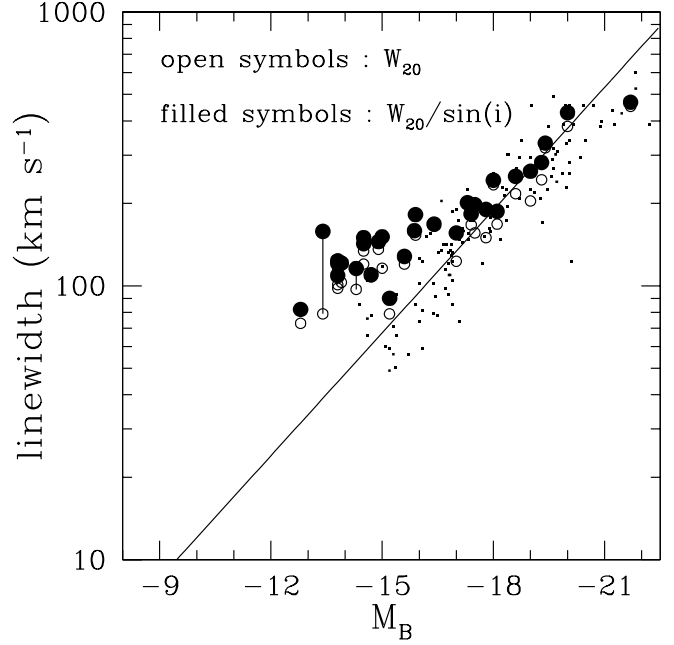


Fig. 3. Luminosity-linewidth relation for the galaxies in the rotation curve sample (large symbols). Open circles represent the measured linewidths before inclination correction; filled circles show the inclination-corrected linewidths. If the open and filled circles are connected by a line, the filled circle is an upper limit only, as explained in the text. The diagonal line is a fit of the TF relation by Kraan-Korteweg et al. (1988) to a sample of nearby galaxies. Small dots are Virgo cluster galaxies used by these authors to study the Tully-Fisher relation for different galaxy types.

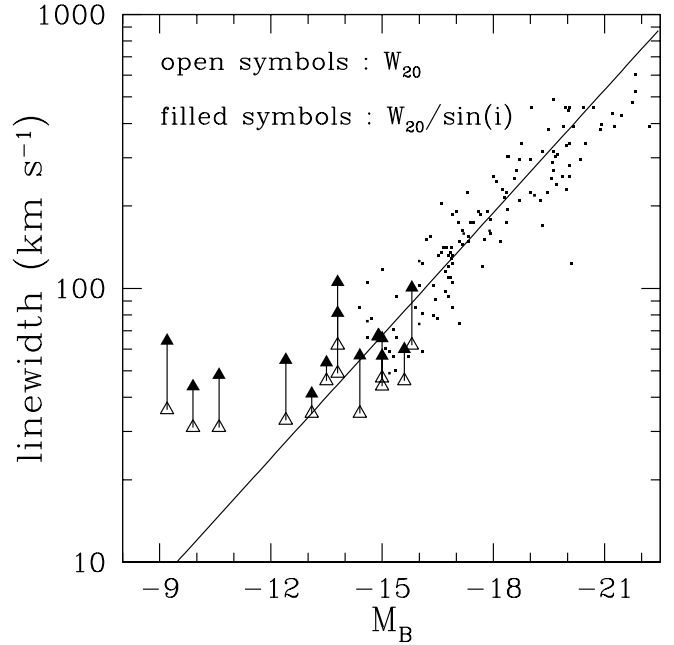


Fig. 4. As Fig. 3, but now for the sample of slow rotators. The open and filled triangles are connected to emphasize the range of plausible inclination corrections as explained in the text.

dwarfs. However, its central HI column density $N_{\text{HI}} = 6.3 \times 10^{21} \text{ cm}^{-2}$ is exceptionally high. In Section 3 we have shown that galaxies with a centrally concentrated HI distribution have linewidths 20% to 30% lower than those with a homogeneous HI distribution. If we consider the maximum rotation velocity instead of the linewidth, DDO 168 is no longer different from the other fast rotators (see Fig. 8). We thus conclude that DDO 168 would have a linewidth comparable to those of the other dwarfs, if it had a smoother HI distribution.

The luminosity-linewidth relation for the slow rotators is shown in Fig. 4. The open and filled triangles are connected in order to emphasize that these are lower and upper limits to the true linewidth Δv_{21} . The mean linewidth W_{20} of the five faintest slow rotators with $M_B > -13$ is $W_{20} = 33.2 \pm 2.3 \text{ km s}^{-1}$, which is the expected value for a non-rotating galaxy with a line of sight velocity dispersion of 9 km s^{-1} . The inclination correction $W_{20}/\sin(i)$ is meaningless for such objects, as is the extrapolation of the T-F relation itself. The more luminous slow rotators follow the extrapolation of the Tully-Fisher relation in the luminosity range $-13 > M_B > -16$, although DDO 75 and DDO 187 (both at $M_B = -13.8$) are relatively far from the T-F relation. Both are observed at a low inclination and DDO 75 may in fact be a fast rotator or an intermediate object. However, the upper limit to the rotation velocity of DDO 187 is 5 km s^{-1} , which classifies it as a slow rotator if the inclination from its observed axial ratio is correct.

We do not argue that dwarf irregular galaxies fall into two distinct categories. In fact, we suggest that DDO 168 is an intermediate object. We checked that the remaining dwarfs in our WSRT sample (Stil & Israel, in preparation) for which a complete rotation curve analysis was not possible, are consistent with the results in Fig. 3 and Fig. 4. The uncorrected linewidths W_{20} of these galaxies cover the range indicated by the fast rotators and the slow rotators. The failure of a complete tilted ring analysis was due to the small size, the small inclination or the near solid-body shape of the rotation curve. The four dwarfs added to Table 1 fall into this category. The RC and SR samples are most likely extremes of a continuous distribution than two separate groups.

The two samples show that low-luminosity dwarf galaxies deviate systematically from the extrapolation of the Tully-Fisher relation for luminous spiral galaxies by being fainter than expected from their linewidth. There are no galaxies in the sample for which the converse is true, i.e. which appear too luminous for their linewidth by a similar amount. However, Kraan-Korteweg et al. (1988) found that the Im type galaxies in their Virgo sample are slightly more luminous than expected from their linewidths.

4.2. Gas content

In Fig. 5 we show the ratio of the actual inclination corrected linewidth to the linewidth predicted by the T-F relation, as a function of gas content measured by the ratio M_{HI}/L_B . Gas-rich dwarf galaxies with $M_{\text{HI}}/L_B > 1 M_{\odot}/L_{B\odot}$ deviate increasingly from the T-F relation with increasing gas content.

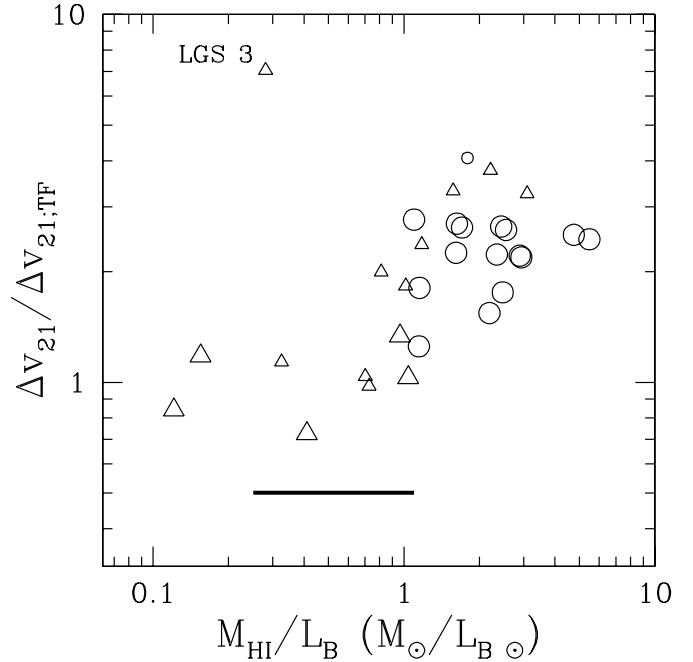


Fig. 5. Ratio of the inclination-corrected linewidth Δv_{21} and the linewidth inferred from luminosity and the T-F relation, as a function of gas content M_{HI}/L_B . Circles indicate the fast rotators, triangles the slow rotators. Objects with inclinations less than 50° are represented by small symbols. The horizontal bar marks the range of M_{HI}/L_B for Sd-Im type galaxies in the sample of Rhee (1996).

The fast rotators are all gas-rich. The gas-rich “slow rotators”, all objects with a small inclination ($i < 50^\circ$), exhibit the same behavior. Note that Δv_{21} values for these galaxies are upper limits to the true linewidth for these galaxies, so that the apparent offset between triangles and circles is not meaningful. Slow rotators less rich in gas ($M_{\text{HI}}/L_B < 1 M_{\odot}/L_{B\odot}$) are consistent with the T-F relation.

This correlation with a parameter which is independent of the distance, shows that the large deviations from the T-F relation found in Section 4.1 cannot be caused by systematic errors in the assumed distance. We have included the three faintest slow rotators in Fig. 5 although the extrapolation of the T-F relation is no longer valid at such low luminosities as it predicts linewidths smaller than expected for HI velocity dispersions of 10 km s^{-1} . This is in fact the cause of the anomalous location of the very faint dwarf galaxy LGS 3 in the diagram.

Finally, we have marked in Fig. 5 by a horizontal bar the M_{HI}/L_B range of Sd-Im galaxies in the sample of Rhee (1996). The fast rotators are mostly outside this range. This explains why large deviations from the T-F relation did not appear in previous studies: fast rotators were not represented in those samples.

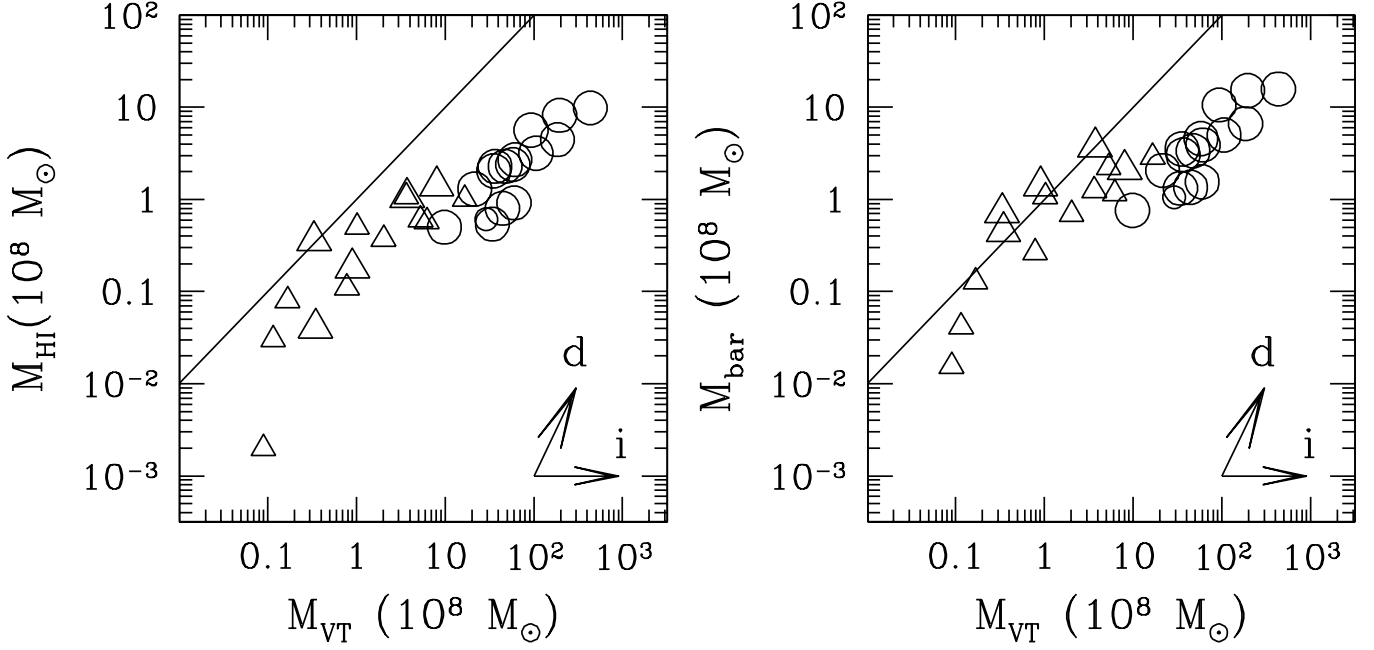


Fig. 6. *Left:* Relation between virial mass and HI mass for the dwarf galaxies in Fig. 9. The solid line is the line of equal mass. Arrows indicate direction and magnitude of errors corresponding to uncertainties of factors of three distance (labeled “d”) and in $\sin(i)$ (labeled “i”), assuming the galaxy is transparent. *Right:* Relation between virial mass and baryonic mass. The slow rotators are dominated by baryonic matter, whereas the fast rotators are dominated by dark matter (Section 4.3).

4.3. Virial and baryonic mass

The total mass within the HI radius R_{HI} follows from the virial theorem (Lo et al. 1993):

$$M_{\text{VT}} = \beta R_{\text{HI}} G^{-1} (V_{\text{rot}}^2 + 3\sigma^2) \quad (3)$$

where σ is the observed line of sight velocity dispersion of the HI. Although the term V_{rot}^2 depends strongly on the inclination, the importance of the isotropic random motions in the slow rotators reduces the errors introduced by the uncertain inclination. The parameter β , of order unity, depends on the actual but poorly known distributions of HI and dark matter. Following Lo et al. (1993), a constant value $\beta = 5/3$ is adopted, corresponding to a homogeneous HI distribution in a halo with a constant density. Although this value does not apply to all of the galaxies discussed here, the systematic error introduced by this is less than a factor 2. This is small compared to the mass range which covers four orders of magnitude.

We adopt the radius of the last measured point of the rotation curve as the radius R_{HI} . The uncertainty in the parameter β is considerably larger than the uncertainty introduced by this approximation.

The baryonic mass is the sum of the gas mass and the stellar mass. The contribution of molecular gas to the overall gas mass in dwarf irregular galaxies is believed to be small. Israel (1997) found the ratio of molecular to atomic hydrogen mass to be about 0.2 for a sample of seven nearby dwarfs. Consequently, we ignore the possible contribution of H_2 . The baryonic mass is then

$$M_{\text{bar}} = (1 + \frac{M_{\text{He}}}{M_{\text{H}}}) M_{\text{HI}} + \left(\frac{M}{L_{\text{B}}} \right)_* L_{\text{B}} \quad (4)$$

where we adopt a ratio of helium to hydrogen $M_{\text{He}}/M_{\text{H}} = 0.3$.

The mass-to-light ratio of the stellar population is calculated from $(B - V)$ colours and the relation (Bottema 1997)

$$\left(\frac{M}{L_{\text{B}}} \right)_* = 1.93 \cdot 10^{0.4(B-V)} - 1.88 \quad (5)$$

The normalization of this relation depends on the poorly known low-mass end of the stellar IMF. However, the strong dependence of the mass-to-light ratio on the colour of the stellar population is taken into account. For a typical object in our sample with $(B - V) = +0.4$, the stellar mass-to-light ratio is 0.91. For the bluest dwarf galaxies, $(B - V) \approx 0$, the derived stellar mass-to-light ratio is very small and much more uncertain. Broeils (1992) found a maximum stellar mass-to-light ratio restricted by the rotation curve in the range 0.5 - 3 for 6 galaxies of type later than Sd.

Fig. 6 shows the relations between HI mass and virial mass, and between baryonic mass and virial mass in the two samples. The difference in virial mass between the slow rotators and the fast rotators is implicit in the sample selection. Although both samples show a correlation between HI mass and virial mass, the slopes are poorly constrained due to the relatively large scatter. A least-squares fit to both samples, excluding the faintest 3 dwarfs with $M_{\text{B}} > -12$, results in the relations

$$\log M_{\text{HI}} = -0.41 + 0.55 \log M_{\text{VT}} \pm 0.27$$

The inverse regression yields

$$\log M_{\text{VT}} = 0.93 + 1.38 \log M_{\text{HI}} \pm 0.42$$

For the relation between baryonic mass and virial mass, we have likewise

$$\log M_{\text{bar}} = -0.14 + 0.41 \log M_{\text{VT}} \pm 0.26$$

$$\log M_{\text{VT}} = 0.66 + 1.59 \log M_{\text{bar}} \pm 0.51$$

All masses are in units of $10^8 M_{\odot}$. The errors are the r.m.s. residuals of the fits. The slope of the fit is sensitive to the treatment of the parameter β . If β is systematically smaller for the fast rotators, the slope of the relation between $\log M_{\text{HI}}$ and $\log M_{\text{VT}}$ is steeper as a function of M_{VT} is steeper than these fits indicate. However, the slope is significantly less than unity for all plausible values of β . Therefore, the lower-mass systems have a larger fraction of their virial mass in gaseous form. For the fast rotators, the virial mass is approximately an order of magnitude larger than the baryonic mass. The fast rotators have velocity gradients within one kpc from the centre of typically $30 \text{ km s}^{-1} \text{ kpc}^{-1}$, about a factor of three larger than those of the slow rotators. This implies central mass densities for the fast rotators approximately an order of magnitude higher than for the slow rotators.

Within the uncertainties introduced by the stellar mass-to-light ratio and the assumptions made to calculate the virial mass, the baryonic mass equals the virial mass for the slow rotators in the luminosity range $-13 > M_{\text{B}} > -16$.

Fig. 7 shows the position of the fast rotators and the slow rotators relative to the T-F relation as a function of baryonic mass. Galaxies from both samples with similar baryonic mass form well-ordered groups in Fig. 7. At similar baryonic mass, the slow rotators tend to be more luminous than the fast rotators because their stellar mass is a larger fraction of the baryonic mass (see also Fig. 5). It is clear from Fig. 7 that the baryonic mass increases along the T-F relation. Qualitatively, this result does not depend on the assumed stellar mass-to-light ratio, but the precise direction in which baryonic mass increases is sensitive to its adopted value.

There is no independent evidence for an evolutionary connection between fast rotators and slow rotators with the same baryonic mass. However, if mass loss due to galactic winds or mergers can be ignored, baryonic mass is conserved in the process of star formation. On the other hand, if a significant amount of gas is expelled in a starburst phase, the total baryonic mass decreases. Therefore, this result places constraints on the evolution of galaxies through star formation in the luminosity-linewidth diagram. We will return to this point.

5. Discussion

5.1. Reality of the deviation

In Section 4.1 we showed that faint dwarf galaxies in general do not follow the extrapolation of the T-F relation established for luminous galaxies. This effect decreases with luminosity and disappears into the scatter in the blue-TF relation near $M_{\text{B}} = -16$. However, a well-defined, surprisingly homogeneous, subclass of faint dwarf galaxies (sample 2) appears to obey the Tully-Fisher relation. Most other dwarf galaxies are

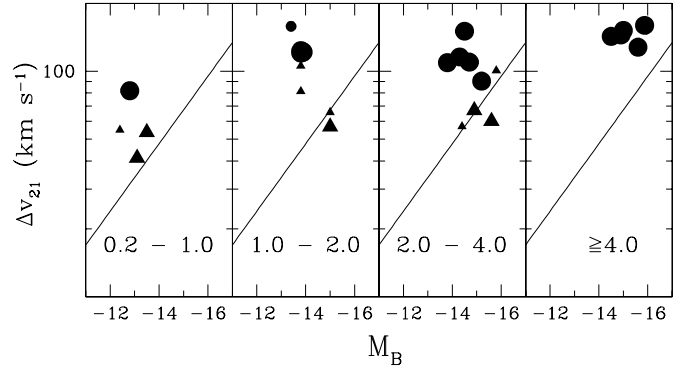


Fig. 7. Position of dwarf galaxies binned by baryonic mass in the luminosity-linewidth diagram. Size and shape of the symbols are as in Fig. 5. Diagonal line represents the Tully-Fisher relation. The ranges in baryonic mass are given in each panel in units of $10^8 M_{\odot}$.

less luminous than expected from their linewidth. The present samples do not contain dwarf galaxies which are overluminous to similar degrees. The largest observed deviation is three magnitudes (factor 15) in luminosity or a factor of two in linewidth. Before we further discuss the result, we consider the possibility that this effect is the result of systematic errors.

There is no systematic error in the linewidth Δv_{21} which could have produced this result. The difference is large, even if we use directly measured linewidths, corrected for instrumental resolution but not for inclination. If the velocity of the flat part of the rotation curve is considered as the velocity parameter of the T-F relation, the linewidth of galaxies with a rotation curve which rises at the last measured point is expected to be *smaller* than its T-F value. A similar argument can be made for the HI distribution, as Δv_{21} cannot exceed the velocity of the HI at the edge of the galaxy, but it can be considerably less if the galaxy has a central concentration of HI.

This leaves the possibility of systematic effects along the luminosity axis. If our result is to be ascribed to distance errors, we must have been underestimating distances systematically by up to a factor of four. Moreover, this systematic distance error must then be luminosity-dependent, because the magnitude of the deviation decreases as the linewidth increases. The argument in Section 4.2, involving high but distance-independent $M_{\text{HI}}/L_{\text{B}}$ ratios (cf. Fig. 5) also argues against this possibility.

We conclude that the extrapolation of the Tully-Fisher relation for luminous galaxies to lower luminosities is not representative for the majority of dwarf galaxies. Dwarf galaxies are on average less luminous than predicted from the width of the 21 cm line and the T-F relation. Such a large deviation from the T-F relation was, in fact, first noticed by Carignan & Beaulieu (1989) for the dwarf galaxy DDO 154 and later by Meurer et al. (1996) for NGC 2915. Both objects have been included in the present sample.

Matthews et al. (1997) found a smaller deviation of 1.3 magnitudes from the Tully-Fisher relation for a large sample of extreme late-type galaxies in the luminosity range $-14.5 >$

$M_B > -16$. This is consistent with the deviation in our RC sample in the same luminosity range. Matthews et al. (1997) also concluded that the baryonic correction was insufficient to place their objects on the T-F relation.

5.2. Origin of the deviation

The basic shape of the T-F relation can be derived from simple arguments (see also Persic 1993 and Zwaan et al. 1995). Assume that the optical radial surface brightness profile is exponential with a central surface brightness Σ_0 and a radial scale length h . The luminosity is $L \sim \Sigma_0 h^2$. This does not exclude a considerable vertical scale height.

The mass within radius R follows from the virial theorem : $M \sim R(v^2 + \sigma^2)$. If the width of the 21 cm HI line is used, R is a fixed point in the rotation curve, unless the rotation curve is flat. Usually, a constant value for the quantity R/h is assumed, and h is eliminated to derive the T-F relation. However, both h and R are fixed by the data and $h \sim R$ is a dubious assumption. If the ratio R/h is explicitly included, the relation between luminosity and velocity is

$$L \sim \frac{\left(\frac{R}{h}\right)^2}{\Sigma_0 \left(\frac{M}{L}\right)^2} (v^2 + \sigma^2)^2 \quad (6)$$

This expression deviates less than 10% from the familiar $L \sim v^4$ for $v > 4\sigma$. Note that R/h and M/L are correlated because M is the mass within radius R .

However, in classic (non-LSB) spiral galaxies with a flat rotation curve, the mass-to-light ratio of the stars can be scaled to explain the inner, rising part of the rotation curve with the stellar mass. The rotation curve of a thin exponential disc is maximal at 2.2 scalelengths (Freeman 1970). Therefore, the linewidth measures the velocity at $R = 2.2 h$, where the luminosity is related to the mass through the mass-to-light ratio within the stellar disc.

Zwaan et al. (1995) showed that LSB galaxies follow the same T-F relation as high-surface-brightness (HSB) galaxies. They inferred the relation $\Sigma_0 \sim (M/L)^{-2}$ as a result of the identical zeropoint of the T-F relations for both high and low surface-brightness galaxies. The inferred correlation between surface-brightness and mass-to-light ratio is confirmed by a detailed comparison between an LSB galaxy and an HSB galaxy at the same position on the T-F relation (De Blok & McGaugh 1996). The LSB galaxies considered by Zwaan et al. (1995) have luminosities $M_B < -15.5$. The ratio between the velocity at 2.2 exponential scalelengths and the velocity at the last measured point of the rotation curve is 0.91 ± 0.11 (data from De Blok 1997). Therefore, the 21 cm HI linewidth is a good representation of the rotation velocity at 2.2 exponential scalelengths. The assumption $R = 2.2 h$ is valid for the LSB galaxies in the sample of Zwaan et al. (1995), even though the stellar disc cannot account for the rotation velocity at this point (De Blok 1997). Therefore, the relationship $\Sigma_0 \sim (M/L)^{-2}$ inferred by Zwaan et al. (1995) is not affected. This also shows

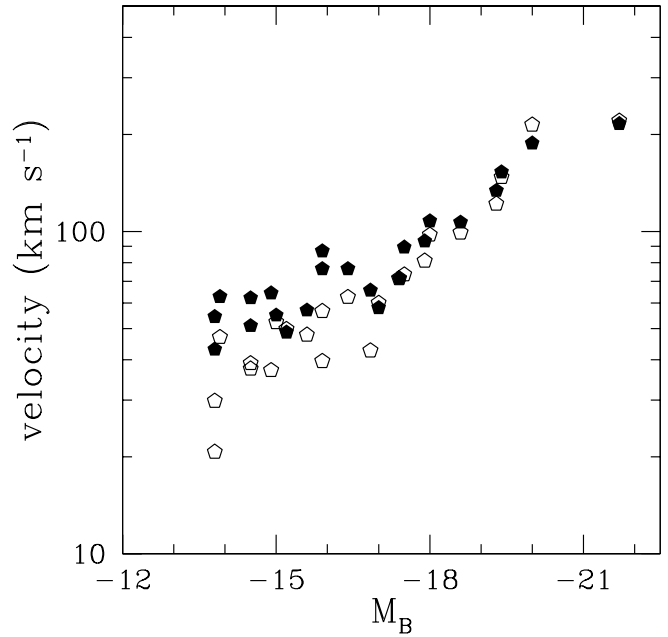


Fig. 8. Tully-Fisher relation for the RC sample in the form of the maximum rotation velocity (filled symbols) and the rotation velocity at 2.2 exponential scalelengths (open symbols) as a function of M_B .

that the relative amplitude of the stellar (partial) rotation curve to the halo (partial) rotation curve is not a critical factor in determining whether a galaxy is on the T-F relation. Therefore, the deviation of dwarf galaxies from the T-F relation should not be interpreted as a breakdown of the so-called “disc-halo conspiracy”.

Thus, the observation that the Tully-Fisher relation for luminous LSB galaxies displays no offset with respect to the T-F relation for HSB galaxies, implies that the product $\Sigma_0 (M/L)^2$ is constant. The observed deviation of the fast rotators is then interpreted as a violation of the assumption $R \sim h$.

The turnover radius of a dwarf galaxy rotation curve can be much larger than the scale length of the optical disc. A detailed analysis of the rotation curves is beyond the scope of this paper, but this can be checked directly for the objects for which mass models exist in the literature (see Table 1). Therefore, the mass measured with the linewidth includes a variable amount of dark matter, depending on the distribution of the HI. This suggests that the deviation of dwarf galaxies from the T-F relation found in Section 4.1 should disappear if the velocity at $R = 2.2 h$ is considered. Fig. 8 shows the maximum velocity (filled symbols) and the velocity at $R = 2.2 h$ (open symbols) as a function of luminosity for the rotation curve sample. As expected, the maximum rotation velocity closely follows the behaviour of the linewidth. As noted before, in this diagram DDO 168 is no longer exceptional. The deviation of the velocity at 2.2 exponential scale lengths is much less, but small deviations remain for the faintest objects. This confirms the importance of the factor R/h in equation (6).

5.3. No evolution

Although the high $M_{\text{HI}}/L_{\text{B}}$ ratio of the fast rotators implies that they have converted relatively little gas into stars, there is no evidence that the fast rotators are presently evolving towards the Tully-Fisher relation. If the star formation rate \dot{M}_* is sufficiently low, old stars are replaced by new stars at a constant, or even diminishing, luminosity. If the stellar rejuvenation timescale $\tau = M_*/\dot{M}_*$ is of the order of the lifetime of the presently most luminous stars, the luminosity of the galaxy does not increase as a result of star formation.

For a dwarf galaxy with luminosity $M_{\text{B}} = -14.5$ ($L_{\text{B}} \approx 10^8 L_{\text{B},\odot}$), and a star formation rate $\dot{M}_* = 0.01 M_{\odot} \text{ yr}^{-1}$, the rejuvenation timescale is $\tau = 10^{10}$ years, i.e. a Hubble time. The star formation rate can barely keep up with the fading of the stellar population, illustrating that a large reservoir of gas does not mean that a galaxy will be more luminous in the future.

However, the observation that the most gas-rich dwarfs are presently underluminous relative to the Tully-Fisher relation justifies a discussion of the possibility that these objects will increase their brightness and become normal Tully-Fisher galaxies in the future.

5.4. Luminosity evolution (the baryonic correction)

The most extreme dwarf galaxies are approximately 2.5 to 3 magnitudes fainter than the T-F luminosity corresponding to their linewidth. Do they contain sufficient amounts of HI to form the stars required to turn them into Tully-Fisher galaxies? We consider a gas-rich dwarf galaxy ($M_{\text{HI}}/L_{\text{B}} = 3$), which is two magnitudes fainter than expected from the T-F relation. If all HI is converted into stars with a stellar mass-to-light ratio $(M/L_{\text{B}})_* = 1$, the galaxy is still a magnitude too faint. This potential luminosity is sometimes called the baryonic correction. Thus, the large luminosity deficiency can only be repaired by creating a stellar population with a very low mass-to-light ratio, which is consequently blue and evolves on a short timescale.

If the mass presently in molecular hydrogen can be neglected (Israel 1997), the HI gas is the reservoir for star formation. The maximum luminosity gain to be achieved corresponds to instantaneous conversion of all HI into stars with a certain mass-to-light ratio. More gradual star formation would produce less luminosity as previous generations of stars fade in the meantime.

If a mass M of gas is converted into stars to obtain a small HI mass-to-blue-light ratio $[M_{\text{HI}}/L_{\text{B}}]_0$, we have

$$\frac{M_{\text{HI}} - M}{L_{\text{B}} + bM} = \left[\frac{M_{\text{HI}}}{L_{\text{B}}} \right]_0$$

with b^{-1} the mass-to-light ratio of the stars. Solving for bM yields the relative increase in luminosity

$$\frac{bM}{L_{\text{B}}} = \frac{b}{1 + b[M_{\text{HI}}/L_{\text{B}}]_0} \left(\frac{M_{\text{HI}}}{L_{\text{B}}} - \left[\frac{M_{\text{HI}}}{L_{\text{B}}} \right]_0 \right) \quad (7)$$

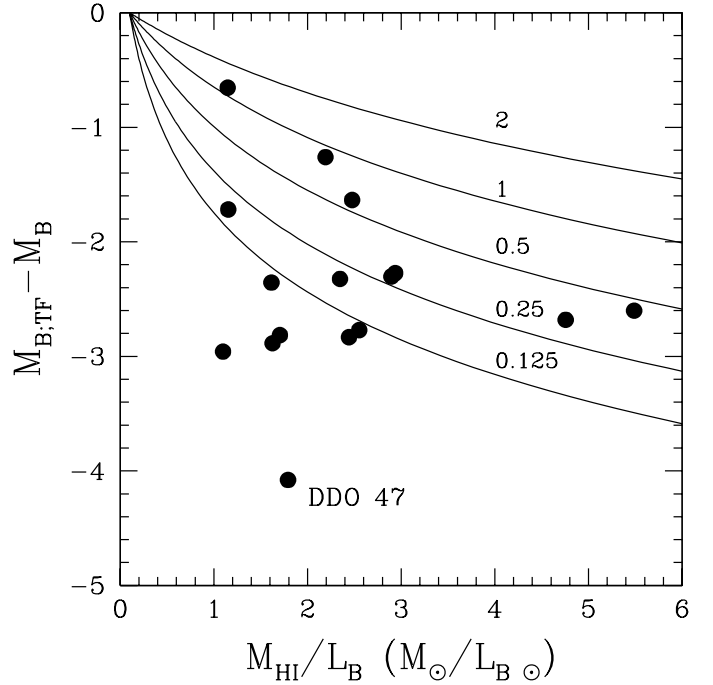


Fig. 9. Deviation of fast rotating dwarfs from the T-F relation as a function of HI gas content. The curves indicate the change in luminosity as a function of initial ratio $M_{\text{HI}}/L_{\text{B}}$, if the HI gas is converted into stars to produce a final ratio $M_{\text{HI}}/L_{\text{B}} = 0.1$, for five possible values of the stellar mass-to-light ratio. A calibration of the T-F relation corresponding to $H_0 = 75 \text{ km s}^{-1} \text{ Mpc}^{-1}$ would shift the points upward by 0.6 magnitudes. The two galaxies with $M_{\text{HI}}/L_{\text{B}} > 4$ are DDO 154 and NGC 2915. The inclination of DDO 47, and therefore its distance from the T-F relation, is very uncertain.

This ratio is shown graphically in Fig. 9 as a function of $M_{\text{HI}}/L_{\text{B}}$ for five values of the mass-to-light ratio $1/b$ of the stellar population. The inferred mass-to-light ratio varies between unity and less than $1/8$ in Fig. 9, but it is sensitive to the adopted calibration of the Tully-Fisher relation. If the zero point of the calibration is shifted from $H_0 = 57 \text{ km s}^{-1} \text{ Mpc}^{-1}$ to $H_0 = 75 \text{ km s}^{-1} \text{ Mpc}^{-1}$, the distance from the TF relation decreases by 0.6 magnitudes. In that case, stellar mass-to-light ratios up to $1/4$ would allow most of the fast rotators to bridge the gap. According to equation (5), stellar mass-to-light ratios between $1/8$ and $1/4$ translate into (B-V) colours between 0 and 0.1, which is considerably bluer than the mean (B-V) of the two samples discussed here. If the normalization of equation (5) yields stellar mass-to-light ratios systematically too low, as suggested by the maximum stellar disc hypothesis, the inferred colours of the stellar population would be even more blue. Therefore, these low stellar mass-to-light ratios are unrealistic.

Observational evidence against luminosity evolution to the T-F relation at constant linewidth is provided by Fig. 7. The baryonic mass of a galaxy on the T-F relation exceeds the mass of a fast rotator with the same linewidth by a factor ~ 3 . This implies that the fast rotators must contain even more gas, which is not detected in single dish measurements of the 21 cm line.

However, if the mass-to-light ratio of the stellar population is much smaller than the normalization of Bottema (1997), the lines of constant baryonic mass would be more horizontal and this problem does not occur. Although very small mass-to-light ratios can increase the baryonic correction, and make it consistent with the distribution of galaxies with similar baryonic mass in the luminosity-linewidth diagram, the blue colours expected for these low mass-to-light ratios are not observed. We therefore conclude that the evolution to the T-F relation at a constant linewidth is unlikely.

5.5. Evolution in linewidth and luminosity

An important constraint for evolution towards the Tully-Fisher relation is in fact given by the same Fig. 7. If we assume that baryonic mass is conserved in the process, evolution in both linewidth and luminosity is consistent with the observed distribution of galaxies with identical baryonic mass in the luminosity-linewidth diagram. If a significant amount of gas, in the order of 50% or more, is lost due to a galactic wind, the distribution of baryonic mass in Fig. 7 also implies a decrease in linewidth.

As the rotation curve is determined primarily by the dark halo, the linewidth can be decreased by transporting gas to the centre, e.g. as the result of tidal interaction with another galaxy. The luminosity is expected to increase as a result of star formation in the high-density gas in the centre.

We test this possibility by assuming that the fast rotators had a low star formation rate $\dot{M}_{*,1}$ for a long period of time, t_1 , similar to LSB galaxies (De Blok 1997), followed by shorter period Δt with a high star formation rate $\dot{M}_{*,2}$ as a result of the concentration of gas towards the centre. Before the starburst, the luminosity of the galaxy is $L_B \approx \dot{M}_{*,1} t_1 / (M/L_B)_{*,1}$. Similarly, the extra luminosity of the stars formed in the burst, is $\Delta L_B \approx \dot{M}_{*,2} \Delta t / (M/L_B)_{*,2}$. We allow for a difference in stellar mass-to-light ratio between the younger and the older stellar population. The ratio of these luminosities is

$$\frac{\Delta L_B}{L_B} = \frac{\dot{M}_{*,2}}{\dot{M}_{*,1}} \frac{\Delta t}{t_1} \mathcal{R} \quad (8)$$

where \mathcal{R} is the ratio of the mass-to-light-ratios of the old and the young stellar population. If the linewidth of a galaxy with a solid body rotation curve is decreased by a factor f , the mean gas surface density increases by a factor f^{-2} . The ratio of the star formation rates follows from the Schmidt (1959) law with an exponent $N = 1.4$ (Kennicutt 1998): $\dot{M}_{*,2}/\dot{M}_{*,1} = f^{-2.8}$. Assume $t_1 = 10^{10}$ yr, $\Delta t = 10^8$ yr (i.e. of the order of the of the orbital timescale of the gas), $(M/L_B)_{*,1} = 1$ and $(M/L_B)_{*,2} = 0.1$. With these assumptions, equation (8) reduces to

$$\frac{\Delta L_B}{L_B} = 0.1 f^{-2.8}$$

For $f = 0.5$ we find $\Delta M_B = -0.6$ magnitudes. Variation of the time of the burst or the mass to light ratio of the stars formed in the burst by a factor of 3 changes ΔM_B by approximately 0.5 magnitudes.

The combination of a decrease in linewidth by a factor 0.5 and an increase in luminosity of 0.6 magnitudes is consistent with the distribution of galaxies with similar baryonic mass in the luminosity-linewidth diagram (Fig. 7).

This mechanism provides both the decrease in linewidth and the higher star formation rate required to move towards the T-F relation. When the baryonic mass becomes more centrally concentrated, the dynamical importance of the halo decreases, and the central galaxy is less dominated by dark matter. The gas from the outer galaxy is expected to be metal-poor, thus providing the possibility of a low-metallicity burst in a galaxy which experienced chemical enrichment in the past.

However, some difficulties remain in this picture. The inner slope of the rotation curve of the fast rotators is considerably larger than that of the slow rotators, implying a higher central mass density in the fast rotators. The published mass models show that this is mainly due to the dark halo. The formation of a central concentration of gas would enhance the density further. Therefore, a fast rotator cannot become a slow rotator similar to those of the present SR sample, unless the density profile of the dark halo is also affected.

We summarize that in principle, there is no reason to suspect that the T-F relation which appears universal for large spiral galaxies, is applicable to dwarf galaxies. Therefore, it remains to be shown that the deviating dwarfs evolve towards the T-F relation. The primary reason to suspect evolution towards the T-F relation is the correlation between M_{HI}/L_B and distance from the T-F relation. However, the baryonic correction, i.e. evolution at a constant linewidth, is inconsistent with the observed large deviations (Matthews et al. 1997 and this work). This leaves the possibility that the T-F relation is applicable only to large spirals and *some* dwarf galaxies (the slow rotators), or that evolution in both linewidth and luminosity occurs. Circumstantial evidence for the latter is provided by the observed ordered distribution of baryonic mass in the luminosity-linewidth diagram.

6. Conclusions.

1. Rotationally supported dwarf galaxies and predominantly pressure supported dwarf galaxies exist together in the luminosity range $-13 > M_B > -16$.

2. The pressure supported dwarf galaxies (the slow rotators) follow the extrapolation of the T-F relation for luminous galaxies. The rotationally supported dwarfs, (the fast rotators) either are systematically too faint or systematically rotate faster than expected from the T-F relation. There is no sharp dichotomy between these extremes.

3. The fast rotators have a larger fraction of gas relative to stars than the slow rotators. Therefore, the fast rotators are less evolved in terms of star formation than the slow rotators. The correlation of gas content with distance from the T-F relation suggests that evolution in the luminosity-linewidth diagram may occur.

4. Within the HI distribution, the dynamics of the fast rotators is dominated by dark matter and of the slow rotators by

baryonic matter (gas and stars). The total mass density (baryonic+dark) is approximately an order of magnitude higher in the fast rotators.

5. The implicit assumption $h \sim R$ (Section 5.2) in the T-F relation is invalid for dwarf galaxies. If the velocity at 2.2 optical scale lengths is considered, as is appropriate for larger spiral galaxies, the deviation of the dwarfs disappears almost completely. A comparison with published results for low-surface-brightness galaxies shows that the larger amplitude of the halo rotation curve, relative to the maximum allowed stellar rotation curve is not the reason of this deviation.

6. Three scenarios for evolution in the luminosity-linewidth diagram were considered : (1). no evolution, (2). evolution in luminosity only, (3). evolution in both luminosity and linewidth. Evolution to the T-F relation in luminosity only is discarded because this requires unrealistically small stellar mass-to-light ratios and because it is inconsistent with the distribution of baryonic mass in the luminosity-linewidth diagram. The deviating dwarf galaxies are either objects which will never be on the T-F relation (no evolution) or evolution in both linewidth and luminosity must occur.

Acknowledgements. This research has made use of the NASA/IPAC Extragalactic Database (NED) which is operated by the Jet Propulsion Laboratory, California Institute of Technology, under contract with the National Aeronautics and Space Administration.

References

- Begeman K.G., 1987, PhD thesis, University of Groningen (NL)
 De Blok W.J.G., McGaugh S.S., 1996, ApJ 469,L89
 De Blok W.J.G., 1997, PhD thesis, University of Groningen (NL)
 Bottema R., 1997, A&A 328,517
 Bottinelli L., Gouguenheim L., Fouqué P., Paturel G., 1990, A&AS 82,391
 Broeils A., 1992, PhD thesis, University of Groningen (NL)
 Burton W.B., Verheijen M.A.W., Kraan-Korteweg R.C., Henning P.A., 1996, A&A 309,687
 Carignan C., Beaulieu S., 1989, ApJ 347,760
 Carignan C., Puche D., 1990 AJ 100,641
 Côté S., Carignan C., Sancisi R., 1991, AJ 102,904
 Côté S., Freeman K., Carignan C., 1997, ASP Conf 117,52
 Freeman K.C., 1970, ApJ 160,811
 Israel F.P., 1997, A&A 328,471
 Jobin M., Carignan C., 1990, AJ 100,648
 Kennicutt R.C., 1998, ApJ 498,541
 Kraan-Korteweg R.C., Cameron L.M., Tammann G.A., 1988, ApJ 331,620
 Kraan-Korteweg R.C., Loan A.J., Burton W.B., Lahav O., Ferguson H.C., Henning P.A., Lynden-Bell D., 1994, Nat 372,77
 Kravtsov A.V., Klypin A.A., Bullock J.S., Primack J.R., 1998, ApJ 502,48
 Lake G., Skillman E.D., 1989, AJ 98,1274
 Lake G., Schommer R.A., Van Gorkom J.H., 1990, AJ 99,547
 Lo K.Y., Sargent W.L.W., Young K., 1990, AJ 106,507
 Matthews L.D., Gallagher J.S., Van Driel W., 1997, ASP Conf. 117, 98
 Meurer G.R., Carignan C., Beaulieu S., Freeman K.C., 1996, AJ 111,1551
 Newton K., 1980, MNRAS 190, 689
 Persic M., 1993, MNRAS 262,392
 Puche D., Carignan C., Bosma A., 1990, AJ 100,1468
 Rhee M.-H., 1996, PhD thesis, University of Groningen (NL)
 Sargent W.L.W., Sancisi R., Lo K.Y., 1983, ApJ 265,711
 Shostak G.S., 1977, A&A 58,L31
 Skillman E.D., Bothun G.D., Murray M.A., Warmels R.H., 1987, A&A 185,61
 Skillman E.D., Terlevich R., Teuben P.J., Van Woerden H., 1988, A&A 198,33
 Schmidt M., 1959, ApJ 129,243
 Staveley-Smith L., Davies R.D., Kinman T.D., 1992, MNRAS 258,334
 Stil J.M., Israel F.P., 1998, in preparation
 Tully R.B., Fisher J.R., 1977, A&A 54,661
 Tully R.B., Bottinelli L., Fisher J.R., Gouguenheim L. Sancisi R., Van Woerden H., 1978, A&A 63,37
 Tully R.B., Fouqué P., 1985, ApJS 58,67
 de Vaucouleurs G., de Vaucouleurs A., Corwin H.G. et al., Third Reference Catalogue, Springer Verlag, N.Y.
 Verheijen, 1997, PhD thesis, University of Groningen (NL)
 Young L.M. & Lo K.Y., 1996, ApJ 462,203
 Zwaan M.A., Van der Hulst J.M., De Blok W.J.G., McGaugh S., 1995, MNRAS 273,L35